PHYSICAL REVIEW A **72**, 052706 (2005)

Theoretical treatment of charge-transfer processes induced by collision of C^{q+} ions with uracil

M. C. Bacchus-Montabonel,[1] M. Łabuda,[1,2] Y. S. Tergiman,[1] and J. E. Sienkiewicz[2]
[1]*Laboratoire de Spectrométrie Ionique et Moléculaire, CNRS et Université Lyon I, 43 Bd. du 11 Novembre 1918, 69622 Villeurbanne Cedex, France*
[2]*Department of Theoretical Physics and Mathematical Methods, Gdańsk University of Technology, ul. Narutowicza 11/12, Pl-80-952 Gdańsk, Poland*

(Received 12 May 2005; revised manuscript received 16 June 2005; published 10 November 2005)

The charge transfer of the RNA base uracil by means of C^{q+} ions ($q=2-4$) has been studied theoretically by means of *ab initio* quantum-chemistry molecular methods followed by a semiclassical dynamical treatment. The charge-transfer process appears to be highly anisotropic. The theoretical cross sections show different behavior with a strong influence of the electronic structure and charge of the C^{q+} projectile and can be correlated positively with previous experimental studies on the ionization and fragmentation processes in the C^{q+}-Uracil collision.

DOI: 10.1103/PhysRevA.72.052706 PACS number(s): 34.70.+e

I. INTRODUCTION

It is well known that the interaction of ionizing radiation with biological tissue can induce severe damage to DNA [1]. The most significant biological consequences are relied to single- and double-strand breaks which appear to be the main underlying mechanisms both for cancer disease and for controlled cell killing used in radiotherapy. It has been shown [2] that important damage is not due to the primary radiation itself, but due to secondary particles generated along the track after the interaction of the ionizing radiation with the biological medium. These particles may be either low-energy electrons, radicals, or singly and multiply charged ions. In that sense, a lot of experiments have been performed recently in order to investigate the action of these secondary particles on biologically relevant molecules. In particular, a great number of studies involving the interaction with low-energy electrons have been undertaken on supercoiled DNA [3], but also on DNA and RNA bases [4,5], as well as on bromouracil [6]. More recently, a number of experimental investigations have been devoted to the action of ions on biomolecules, generally at relatively low collisional energies in the range [2–150] keV. In particular, coincidence measurements between outgoing projectiles have been carried out in collisions of C^{q+} ions on uracil [7] or thymine [8] with analysis of the fragment mass distribution by time-of-flight spectrometry. A similar experimental procedure has been used for recent studies of F^{2+} on adenine [9] or proton on uracil [10]. Higher-charged ions have also been investigated at higher energies [11,12].

In such low-energy collisions between biomolecule and ions, different processes may be considered: excitation and fragmentation of the biomolecule, ionization of the gaseous target, and also possible charge transfer from the multicharged ion towards the biomolecule. From the experimental point of view, excitation and fragmentation processes have been mainly investigated and the peak integration of the mass spectra as a function of the collision velocity leads to an evaluation of the relative cross sections for the different ionization and fragmentation channels. In a recent study of keV collisions of C^{q+} ions with uracil [7], in particular, a strong influence of the electronic structure and charge q ($q=1-6$) of the C^{q+} ion on the ionization and fragmentation processes was observed. At low velocities, almost complete fragmentation has been observed for the C^{2+} projectile ion, whereas for all the other projectile charge states the induced fragment yield is markedly lower. Furthermore, a rather complete shattering of the ring has been observed, instead of a single-atom abstraction from the biomolecule. Similar experiments on thymine [8] show a strong dependence of the fragment kinetic energies on the fragment initial location within the parent molecule. Such experimental results focused on the fragmentation process cannot give any information on possible charge transfer, which should be, however, a complementary process to fragmentation. In order to have a more complete understanding of the different mechanisms and electronic structure of the projectile and target involved in these reactions, we have undertaken a theoretical study of the charge-transfer process for a series of charge $q=[2-4]$ of the C^{q+}+uracil system using an *ab initio* molecular calculation of the potential energies and corresponding coupling matrix elements followed by a semiclassical dynamics in the [3–150] keV collision velocity range where experimental data are available. To our knowledge, no theoretical approaches for such collisional systems are available.

II. MOLECULAR CALCULATIONS

A. Molecular model

A simple model of this polyatomic complex collisional system may be proposed by means of the one-dimensional reaction coordinate approximation widely used in a number of cases [13,14]. Effectively, the collision may be represented as the evolution of the polyatomic $C^{q+}\cdots$uracil complex which, in a first approximation, could be treated as a pseudodiatomic system, the reaction coordinate corresponding to the distance between the center of mass of the uracil molecule and the colliding carbon ion. The rearrangement of the uracil molecule when approaching the C^{q+} ion can be

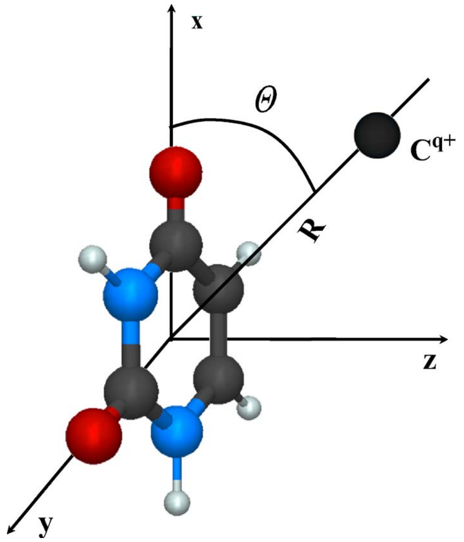

FIG. 1. (Color online) Internal coordinates for the C^{q+}+uracil system.

taken into account by relaxation of the geometry of the uracil-C^{q+} complex along the reaction path. Of course, such an approach does not consider the degrees of freedom of the complex and the internal motions of the molecule, but it seems reasonable in a very fast collisional process where nuclear vibration and rotation periods are assumed to be much longer than the collision time.

In such a problem, different molecular states of the C^{q+}-uracil collisional system are involved and the potentials may be calculated along the reaction coordinate R for different approaches θ from perpendicular ($\theta=90°$) to planar geometry ($\theta=0°$) (Fig. 1) in order to take into account the anisotropy of the process. This requires, of course, extensive calculations. In a first step, we have focused our attention on the two limit cases, corresponding to the perpendicular ($\theta=90°$) and planar attack ($\theta=0°$) of the carbon ion on the uracil molecule, in order to take care of the different geometrical configurations and angle averaging.

No symmetries are included for the perpendicular collisional process; the calculations have been performed using Cartesian coordinates with origin of coordinates at the center of mass of the uracil molecule. On the contrary, a plane of symmetry can be considered for the planar attack and calculations have been performed using the C_s symmetry group. In that case, all the collision directions in the plane of the molecule should be theoretically considered; nevertheless, a great number of complexes between the uracil molecule and a series of single- or double-charged ions have been investigated already. The optimized structures and attachment sites have been calculated, for example, for the alkali-metal Li^+ [15], Na^+, and K^+ cations [16], as well as alkaline-earth-metal Mg^{2+}, Ca^{2+} [17], and Mn^{2+} double-charged ions [18] or copper (I) ion [19,20]. These studies show for the different metal ions a minimum energy for the metal-uracil complex corresponding to an attachment site on oxygen O(4) (see Fig. 2) which appears to be a preferential site. In a first approach, we have thus considered the collisional attack of the carbon ion C^{q+} along the C(4)-O(4) direction, corresponding to the angle $\theta=0°$, for the series of charges $q=[2-4]$.

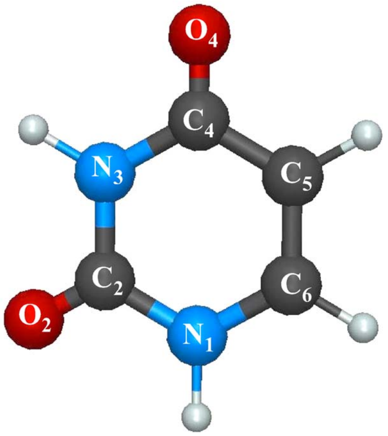

FIG. 2. (Color online) Geometry of the uracil molecule.

The collision dynamics has been treated by a semiclassical approach in the framework of the sudden approximation hypothesis which assumes the electronic transition to occur so fast that the vibrorotation motion stays unchanged. The molecular vibration is thus ignored, and the ion-molecule collision may be visualized as an ion bumping into an anisotropic atom. This is, of course, a first-order level of approximation, but it has shown its efficiency in a number of ion-diatomics collisions [21–24] in the energy range we are dealing with. In that sense, it appears that, at these collision energies, the charge-transfer mechanism may be induced by very fast electronic transitions and the uracil molecule can be considered as frozen during the process.

B. Molecular results

Molecular calculations were carried out using the MOLPRO suite of *ab initio* programs [25]. The radial coupling matrix elements between all pairs of states of the same symmetry have been calculated by means of the finite-difference technique:

$$g_{KL}(R) = \langle \psi_K | \partial/\partial R | \psi_L \rangle = \lim_{\Delta\to 0} \frac{1}{\Delta} \langle \psi_K(R) | \psi_L(R+\Delta) \rangle,$$

with the parameter $\Delta=0.0012$ a.u. as previously tested and using the three-point numerical differentiation method for reasons of numerical accuracy. The center of mass of the uracil molecule has been chosen as the origin of the electronic coordinates.

The geometry of the ground state, as well as singly and doubly ionized uracil molecules, has been optimized by means of density-functional-theory (DFT) calculations using the Beck-Lee-Yang-Parr density functional (B3LYP) which has been shown to be computationally efficient and provides accurate structures and transition energies [26]. The vertical and adiabatic first and second ionization potentials have thus been determined. They are presented in Table I and compare favorably to previous calculations [27,28] and experimental data [29,30].

TABLE I. Ionization potentials of the uracil molecule (in eV).

	This calculation B3LYP/6-31G**	Russo *et al.* [27] B3PW91	Crespo-Hernandez *et al.* [28] PMP2/6-31++G(d,p)	Experiment
PI1: $U \rightarrow U^+$ vertical	9.56		9.43	9.50 [29]
PI1: $U \rightarrow U^+$ adiabatic	9.34	9.32 TZVP 9.33 6-311++G**	9.36	9.32 [29] 9.35 [30]
PI2: $U^+ \rightarrow U^{2+}$ vertical	17.57			
PI2: $U^+ \rightarrow U^{2+}$ adiabatic	17.33			

1. In-plane collisional attack

In that case, the collisional system presents a plane of symmetry, and calculations have been performed in the C_s symmetry group with consideration of a planar approach along the C(4)-O(4) chemical bond corresponding to the x axis. Spin-orbit coupling being negligible in the energy range of interest, we can assume the electron spin to be conserved in the collision process and only the A' states involved in the process have been considered. The A'' states have not been taken into account, as they can be involved only by means of rotational coupling. Calculations have thus been performed for singlet states in the case of $C^{2+}(1s^2 2s^2)$ and $C^{4+}(1s^2)$ projectile ions and for doublet states in the case of $C^{3+}(1s^2 2s)$ cations. The molecular orbitals were optimized in state-average complete active space self-consistent field (CASSCF) calculations using the 6-31G^{**} basis set of atomic orbitals. The active space includes the five highest valence orbitals, including the $n=2,3$ levels of the colliding carbon atom which might be involved in the process. The corresponding 1s orbital has been treated as frozen core.

a. $C^{2+}(1s^2 2s^2)$+*uracil system.* The potential energy curves and radial coupling matrix elements have been calculated for a distance C^{2+}-O(4) varying from 0.5 to 5 Å. The charge-transfer levels are presented in Fig. 3(a). They can be described as an excitation from the a'' molecular orbitals (called by extension π as they are perpendicular to the xy uracil plane) to the $2p_z$ orbital centered on the colliding carbon; no excitation appears between the a' orbitals, the highest one corresponding to the $2p_x$ orbital centered on O(2) staying doubly occupied. Such potential energy curves show clearly avoided crossings in the 1.5–2.0-Å range corresponding to a strong interaction with the entry channel $C^{2+}(1s^2 2s^2)$+uracil corresponding to the configuration $\{(p^x_{O(2)})^2(\pi_{C(2)O(2)})^2(\pi_{C(4)O(4)})^2(\pi_{C(5)O(6)})^2\}$ [only the highest occupied molecular orbitals (HOMO's) of the complex are specified—27 doubly occupied molecular orbitals are implicit] with a doubly occupied orbital on O(2) in the attack axis x. In this process, we observe clearly a single charge transfer from a π electron of the highest occupied molecular orbital of the uracil ring $\pi_{C(5)C(6)}$ to the unoccupied $2p_z$ orbital of the projectile carbon ion to lead to the ${}^1A'_1\{C^+(1s^2 2s^2 2p_z)+U^+\}$ level. At increasing energy, this process is associated with π-π excitations of the out-of-plane (a'' symmetry) $\pi_{C(2)O(2)}$ and $\pi_{C(4)O(4)}$ orbitals to the $\pi_{C(5)O(6)}$ orbital leading to the excited $\{C^+(1s^2 2s^2 2p_z)+U^{+^*}\}$ ${}^1A'_2$ and ${}^1A'_3$ molecular charge-transfer levels. Double capture may also be observed with capture of two π electrons of the ring without internal excitation leading to the ${}^1A'_4\{C(1s^2 2s^2 2p_z^2)+U^{2+}\}$ state. The evolution of the electronic structure with the C^{2+}-O(4) internuclear distance may be visualized qualitatively by means of the electronic density and Mulliken population analysis. The electronic densities on the lowest charge-transfer level ${}^1A'_1$ are presented in Fig. 4 for the three internuclear distances 3, 2, and 1 Å. No interaction appears at 3 Å between the C^+ and ionized U^+ ions, which can be considered as separated in the asymptotic internuclear distance region; on the contrary, a delocalization of the electrons towards the projectile is visualized at 2 Å, leading to a real chemical bond at 1 Å. Such a delocalization of the π electrons of the uracil ring towards the C^+ ion is also observed on the Mulliken population analysis (Fig. 5): the charge on the colliding carbon is 1+ at long range on the different molecular states, corresponding to a C^+/U^+ system, and decreases with the internuclear distance, showing the delocalization of the electrons of the ring.

b. $C^{3+}(1s^2 2s)$+*uracil system.* The potentials and radial couplings have been calculated in the same internuclear distance range from 0.5 to 5 Å as for C^{2+}-uracil. The charge-transfer levels are presented in Fig. 3(b) and show similarly avoided crossings in the 1.5–2.0-Å range which can be attributed to an interaction with an entry channel corresponding to the $\{(p^x_{O(2)})(\pi_{C(2)O(2)})^2(\pi_{C(4)O(4)})^2(\pi_{C(5)C(6)})^2\}$ configuration (same conventions as above) which may be attributed to the ionized uracil molecule U^+ and $C^{2+}(1s^2 2s^2)$ ion collisional system. There is in fact delocalization of an electron from an a' orbital centered on uracil to the $2s$ (a' symmetry) orbital on the colliding carbon, leading to a doubly occupied $2s$ level $C^{2+}(1s^2 2s^2)$. The process is then the same as previously, with excitation from the a'' molecular orbital $\pi_{C(5)C(6)}$ to the $2p_z$ orbital of the colliding carbon corresponding to the ${}^1A'_1\{C^+(1s^2 2s^2 2p_z)+U^{2+}\}$ state and, at higher energy, π-π excitations between the $\pi_{C(4)O(4)}$ and $\pi_{C(5)C(6)}$ out-of-plane orbitals, leading to the $\{C^+(1s^2 2s^2 2p_z)+U^{2+*}\}{}^1A'_2$ state.

(*c*) $C^{4+}(1s^2)$+*uracil system.* The features appear somewhat different in that case. The potential energy curves charge transfer levels are presented in Fig. 3(c). They show avoided crossings slightly displaced towards 2.0 Å to be attributed to

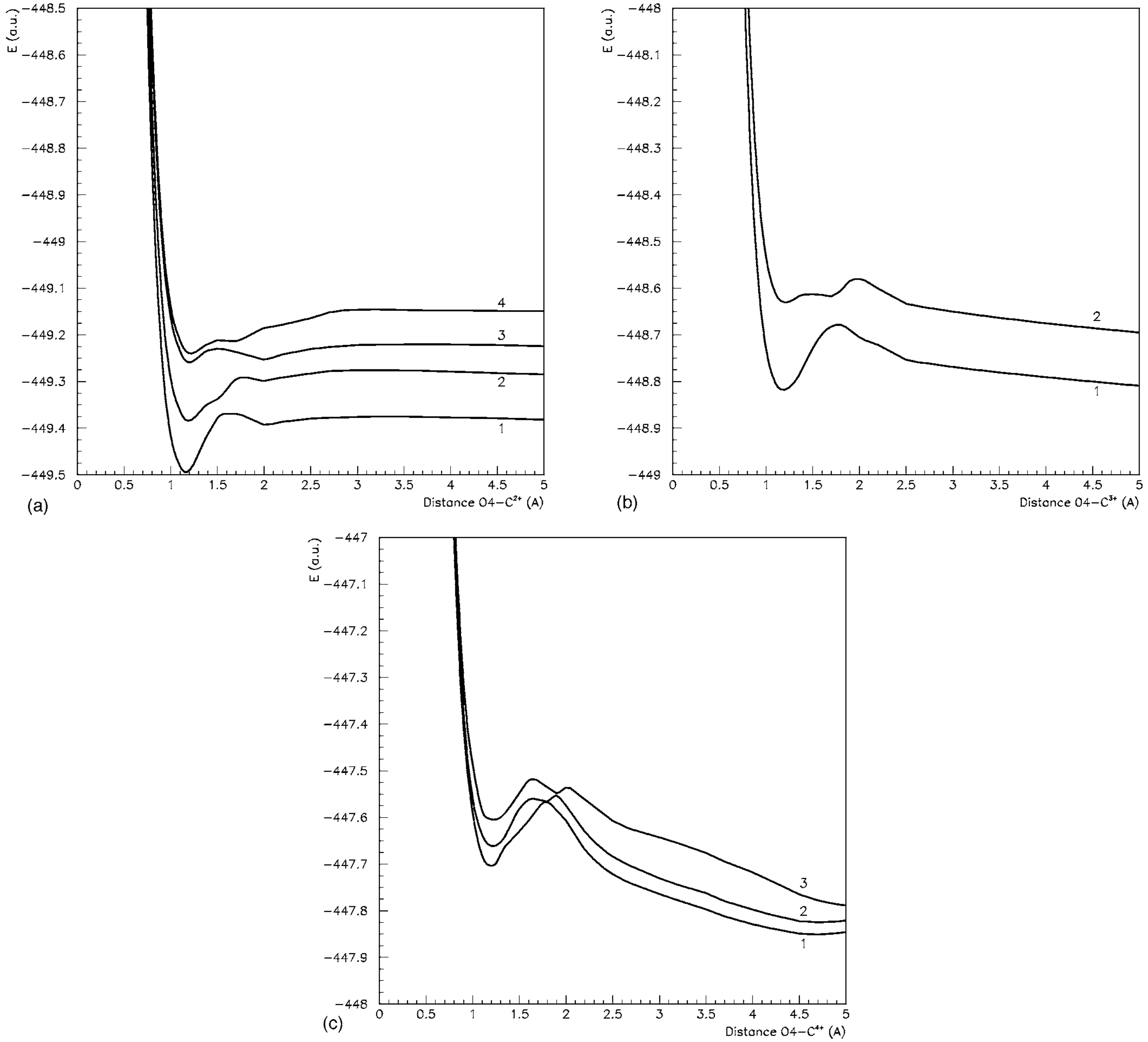

FIG. 3. (a) Adiabatic potential energy curves for the charge-transfer levels of the C^{2+}-uracil collisional system in the planar attack. 1: $^1A'$ state corresponding to the configuration $\{(p^x{}_{O(2)})^2(\pi_{C(2)O(2)})^2(\pi_{C(4)O(4)})^2\pi_{C(5)C(6)}2p_z\}$. 2: $^1A'$ state corresponding to the configuration $\{(p^x{}_{O(2)})^2(\pi_{C(2)O(2)})^2(\pi_{C(4)O(4)})(\pi_{C(5)C(6)})^2 2p_z\}$. 3: $^1A'$ state corresponding to the configuration $\{(p^x{}_{O(2)})^2(\pi_{C(2)O(2)}) \times(\pi_{C(4)O(4)})^2(\pi_{C(5)C(6)})^2 2p_z\}$. 4: $^1A'$ state corresponding to the configuration $\{(p^x{}_{O(2)})^2(\pi_{C(2)O(2)})^2(\pi_{C(4)O(4)})^2 2p_z{}^2\}$. (b) Adiabatic potential energy curves for the charge-transfer levels of the C^{3+}-uracil collisional system in the planar attack. 1: $^2A'$ states corresponding to the configuration $\{p^x{}_{O(2)}(\pi_{C(2)O(2)})^2(\pi_{C(4)O(4)})^2\pi_{C(5)C(6)}2p_z\}$. 2: $^2A'$ states corresponding to the configuration $\{p^x{}_{O(2)}(\pi_{C(2)O(2)})^2(\pi_{C(4)O(4)}) \times(\pi_{C(5)C(6)})^2 2p_z\}$. (c) Adiabatic potential energy curves for the charge-transfer levels of the C^{4+}-uracil collisional system in the planar attack. 1: $^1A'$ state corresponding to the configuration $\{p^x{}_{O(2)}2p_x(\pi_{C(2)O(2)})^2(\pi_{C(4)O(4)})^2\}$. 2: $^1A'$ state corresponding to the configuration $\{p^x{}_{O(2)}2p_x(\pi_{C(2)O(2)})^2\pi_{C(4)O(4)}\pi_{C(5)C(6)}\}$. 3: $^1A'$ state corresponding to the configuration $\{p^x{}_{O(2)}2p_x\pi_{C(2)O(2)}(\pi_{C(4)O(4)})^2\pi_{C(5)C(6)}\}$.

an interaction with an entry channel corresponding to the $\{(p^2_{O(2)})^2(\pi_{C(2)O(2)})^2(\pi_{C(4)O(4)})^2\}$ configuration (same conventions as above). As for C^{3+}+uracil, there is delocalization of electrons, two in that case, from an a' orbital centered on uracil to the $2s$ (a' symmetry) orbital on the colliding carbon to lead to the $\{C^{2+}(1s^2 2s^2)+U^{2+}\}$ collisional system, but the charge-transfer mechanism appears to be different, as it proceeds now with a single capture from an electron of the a' orbital $p^x_{O(2)}$ to the p_x orbital on the colliding carbon along the x direction leading to the $^1A'_1\{C^{+}(1s^2 2s^2 2p_x)+U^{3+}\}$ channel. At increasing energies, there are still π-π excitation between the out-of-plane $\pi_{C(2)O(2)}$ and $\pi_{C(4)O(4)}$ orbitals towards $\pi_{C(5)C(6)}$ corresponding respectively to the $^1A'_2$ and $^1A'_3\{C^{+}(1s^2 2s^2 2p_x)+U^{3+*}\}$ levels. In all cases, the Mulliken

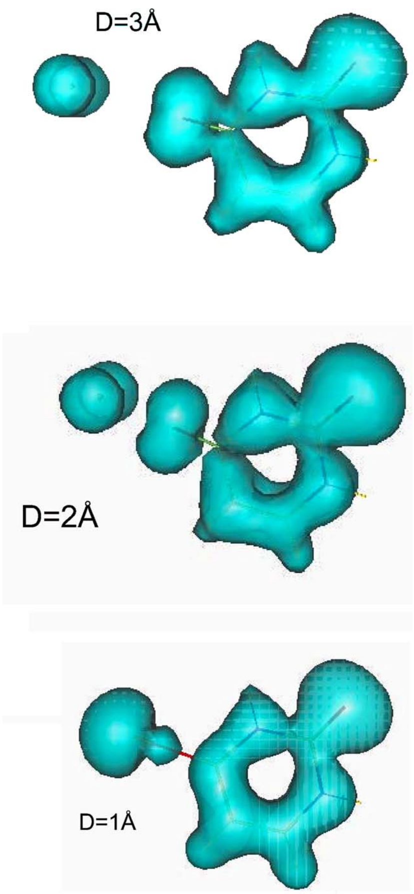

FIG. 4. (Color online) Electronic density of the $^1A_1'$ state of the C^{2+}+uracil system.

population analysis shows that the electronic molecular levels correspond to a charge around 1+ on the colliding carbon at long range, attributed to the $C^+(1s^22s^22p)$ ion.

2. Perpendicular collisional attack

For perpendicular collisions, no symmetry can be considered and calculations have been performed using Cartesian coordinates with origin of coordinates at the center of mass of the uracil molecule, the colliding ion lying along the z axis and the uracil molecule being in the xy plane. The active space takes into account the p_x, p_y, and p_z components of the $2p$ orbitals centered on the oxygen atoms, the $\pi_{C(5)C(6)}$ orbital, and the $2p_x$, $2p_y$, and $2p_z$ orbitals of the colliding ion.

a. $C^{2+}(1s^22s^2)$+*uracil system.* The potentials and radial couplings have been calculated for a distance R varying from 0.5 to 5 Å. The potential energy curves are presented in Fig. 6(a). As in the planar attack, we observe an interaction around 2 Å with the entry channel $C^{2+}(1s^22s^2)$+uracil corresponding to the configuration $\{(2p_O)^2(\pi_{C(5)C(6)})^2\}$ with a doubly occupied orbital $2p_O$ along the z axis [the $2p_O$ orbital is a linear combination of the $2p_z$ orbitals of atoms O(2) and O(4)—29 doubly occupied molecular orbitals including the π_{CO} orbitals on C(2)O(2) and C(4)O(4) are implicit]. The charge-transfer process proceeds with excitation of an electron of the $\pi_{C(5)C(6)}$ orbital of the uracil to the unoccupied $2p$ orbital of the projectile carbon ion, but in that case, three states have to be considered for the $\{C^+(1s^22s^22p)+U^+\}$ configuration, corresponding to the three $2p_x$, $2p_y$, and $2p_z$ components of the $2p$ level of the colliding carbon. Contrary to the planar attack where delocalization between the $2p_z$ orbital on carbon and the out-of-plane orbitals was favored, the interaction is now smothered for the $2p_z$ component centered at the center of mass of the uracil molecule which presents a lower overlap with π_{CO} and π_{CC} orbitals than the $2p_x$ and $2p_y$ components. As already observed in the planar attack, double excitation of the $\pi_{C(5)C(6)}$ electrons to the $2p_z$ orbital of the colliding carbon may be observed leading to the $\{C(1s^22s^22p_z^2)+U^{2+}\}$ level.

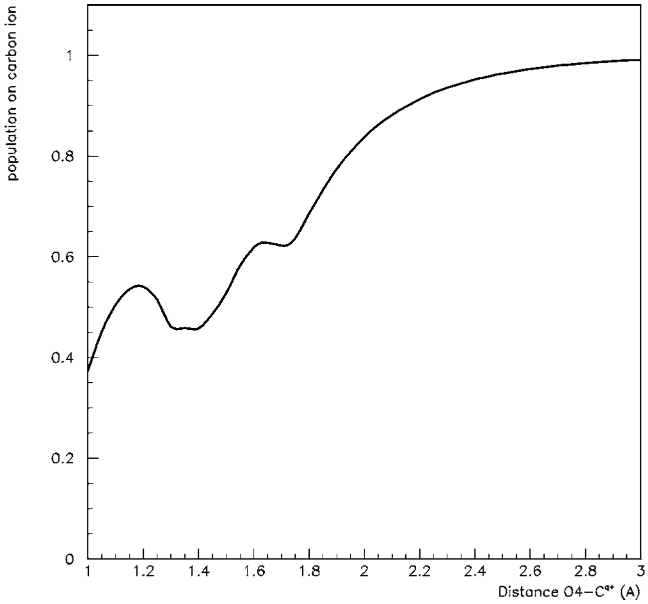

FIG. 5. Mulliken population analysis for the $^1A_1'$ level of the $C^{2+}(1s^22s^2)$+uracil collisional system.

b. $C^{3+}(1s^22s)$+*uracil system.* The potential energy curves are presented in Fig. 6(b). Similarly to the in-the-plane collision, a delocalization of an electron from an orbital centered on uracil to the $2s$ orbital of the colliding carbon is observed leading to charge-transfer levels corresponding to the $\{C^+(1s^22s^22p)+U^{2+}\}$ configuration. The three states correspond to an excitation of an electron of the $\pi_{C(5)C(6)}$ orbital of the uracil to the $2p_x$, $2p_y$, and $2p_z$ components of the unoccupied $2p$ orbital of the colliding atom with an unpaired electron on the $2p_O$ orbital. They are degenerated at long range, and almost no interaction may be noticed except a shift in energy around $R=2$ Å.

c. $C^{4+}(1s^2)$+*uracil system.* In that case, the molecular calculations have been performed until 9 Å in order to describe the avoided crossing around 6 Å between the entry channel $^1A_4$ and the excited charge-transfer levels $^1A_5$, $^1A_6$, and $^1A_7$. As previously stated, there is delocalization of two electrons of the uracil molecule leading to the $\{C^{2+}(1s^22s^2)+U^{2+}\}$ system corresponding to the $\{(2p_O)^2\}$ configuration with a doubly occupied orbital in the z attack axis. The main process is, as in the planar collision, an excitation of an electron of the $2p_O$ orbital on oxygen to the $2p$ orbital of the colliding car-

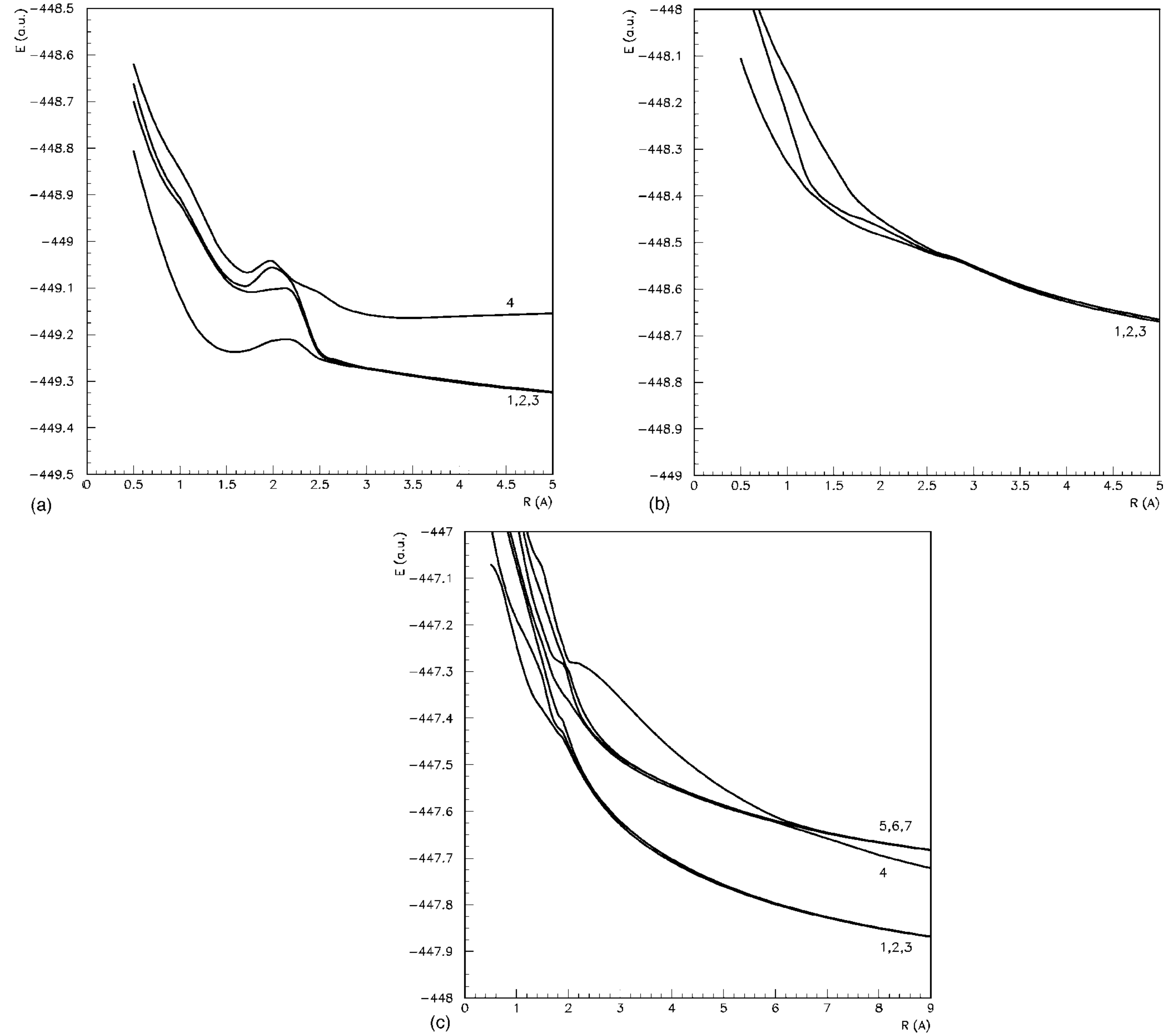

FIG. 6. (a) Adiabatic potential energy curves for the charge-transfer levels of the C^{2+}-uracil collisional system in the perpendicular attack (numbering by increasing energy). 1: ^1A state corresponding to the configuration $\{(2p_O)^2\pi_{C(5)C(6)}2p_z\}$. 2: ^1A state corresponding to the configuration $\{(2p_O)^2\pi_{C(5)C(6)}2p_y\}$. 3: ^1A state corresponding to the configuration $\{(2p_O)^2\pi_{C(5)C(6)}2p_x\}$. 4: ^1A state corresponding to the configuration $\{(2p_O)^2 2p_z^2\}$. (b) Adiabatic potential energy curves for the charge-transfer levels of the C^{3+}-uracil collisional system in the perpendicular attack (numbering by increasing energy). 1: ^1A state corresponding to the configuration $\{2p_O\pi_{C(5)C(6)}2p_z\}$. 2: ^1A state corresponding to the configuration $\{2p_O\pi_{C(5)C(6)}2p_y\}$. 3: ^1A state corresponding to the configuration $\{2p_O\pi_{C(5)C(6)}2p_x\}$. (c) Adiabatic potential energy curves for the charge-transfer levels of the C^{4+}-uracil collisional system in the perpendicular attack (numbering by increasing energy). 1: ^1A state corresponding to the configuration $\{2p_O2p_z\}$. 2: ^1A state corresponding to the configuration $\{2p_O2p_y\}$. 3: ^1A state corresponding to the configuration $\{2p_O2p_x\}$. 4: ^1A state corresponding to the configuration $\{(2p_O)^2\}$. 5: ^1A state corresponding to the configuration $\{\pi_{C(5)C(6)}2p_z\}$. 6: ^1A state corresponding to the configuration $\{\pi_{C(5)C(6)}2p_y\}$. 7: ^1A state corresponding to the configuration $\{\pi_{C(5)C(6)}2p_x\}$.

bon ion, with, as noticed in the C^{2+}+uracil system, a stronger interaction for the $2p_x$ and $2p_y$ components. An additional $2p_O \rightarrow \pi_{C(5)C(6)}$ excitation may be considered also leading to the $\{C^+(1s^22s^22p)+U^{3+*}(\pi_{C(5)C(6)})\}$ levels. Compared to the C^{3+}+uracil and even the C^{2+}+uracil systems, strong avoided crossings are observed in that case between the charge-transfer levels and the entry channel, which should induce certainly significant charge-transfer cross sections.

As a summary of this molecular study, it appears clearly that in all these molecular systems, we are dealing with a $C^{2+}(1s^22s^2) \rightarrow C^+(1s^22s^22p)$ process, corresponding to an excitation of an electron from the uracil molecule ($\pi_{C(5)C(6)}$ for C^{2+} and C^{3+} and $2p_O$ for C^{4+}) to the $2p$ orbital on the colliding carbon ion. This is confirmed by the Mulliken population analysis, which, in all cases, shows that the charge-transfer molecular levels correspond to a charge

TABLE II. Charge-transfer cross sections for the series of C^{q+}-uracil, $q=[2-4]$, collisional systems (in 10^{-16} cm^2).

Velocity (a.u.)	Lab. energy (keV)	Planar collision			Perpendicular collision	
		$C^{2+}+U$	$C^{3+}+U$	$C^{4+}+U$	$C^{2+}+U$	$C^{4+}+U$
0.1	3	0.0098	0.327	0.099	0.002	7.558
0.2	12	0.175	0.128	0.112	0.003	8.081
0.3	27	0.209	0.059	0.123	0.004	5.702
0.4	48	0.165	0.034	0.142	0.006	6.655
0.5	75	0.123	0.022	0.211	0.010	7.195
0.6	108	0.093	0.015	0.215	0.022	6.798
0.7	147	0.072	0.011	0.247	0.070	6.033

around 1+ on the colliding carbon at long range, attributed to $C^+(1s^2 2s^2 2p)$. The uracil molecule appears as an electron reservoir which fills up the electron deficit of the colliding ion by delocalization of the electrons of the uracil ring towards the carbon projectile. This suggests, in agreement with previous experimental observations on ion-molecule collisional systems [31], that we can expect in such processes a strong electronic rearrangement with the predominance of multielectron capture from the electronic cloud of the uracil molecule towards the C^{q+} colliding ion for $q>2$, although a single-capture mechanism is observed for $q=2$. In spite of important anisotropic effects, such a mechanism is observed in both planar and perpendicular collisions and may drive different dynamics for the different charges q of the projectile in the C^{q+}-uracil reactions.

III. COLLISION DYNAMICS

The collision dynamics of the charge-transfer process has been performed in the $[0.1-0.7]$ a.u. collision velocity range ($[3-147]$ keV laboratory energies) corresponding to the same impact energies as the fragmentation experiments [7]. In this energy domain, semiclassical approaches using the EIKONXS code based on an efficient propagation method [32] may be used with a good accuracy. All the transitions between states of the same symmetry, driven by radial coupling matrix elements, have been considered for the series of colliding C^{q+} $q=[2-4]$, carbon ions. As previously stated, rotational couplings have not been taken into account in this calculation. The center of mass of the uracil molecule has been taken as the origin of the electronic coordinates. The coupled equations have been solved with a step size such that an accuracy of 10^{-4} for the symmetry of the S matrix is achieved. We have explored impact parameters between 1.0 and 10.0 a.u. The results for the planar and perpendicular collisions are presented in Table II. For the C^{2+}-uracil collision system, there is clearly a strong increase of the charge-transfer cross section with increasing velocity, at low energies, for the collision in the plane of the uracil molecule. We observe also a regular increase of the charge-transfer cross sections in the case of the perpendicular attack, but the values remain always very small. The behavior of the other colliding species appears quite different. The C^{4+}-uracil collision system shows only small variations of charge-transfer cross sections with velocity, around $[0.1-0.25]\times 10^{-16}$ cm^2 in the planar collisional attack. On the contrary, in the perpendicular collision, the charge-transfer cross sections reach values around $6-8\times 10^{-16}$ cm^2, in relation with the strong avoided crossings observed on the molecular structure calculations. The main contribution is related to the interaction of the entry channel with the excited $\{C^+(1s^2 2s^2 2p)+U^{3+*}(\pi_{C(5)C(6)})\}$ channels, in particular the states corresponding to the p_x and p_y levels of the colliding carbon ion. In that case, the collision process is completely anisotropic and the orientation of the projectile with regard to the uracil molecule is determinant with differences of at least one order of magnitude. The C^{3+}-uracil collision systems shows a regular decrease of the charge-transfer cross section with increasing velocity in the planar collision, but no significant charge-transfer process may be considered in the perpendicular attack.

The average of the cross sections for both planar and perpendicular collision attacks have been determined to compare with the experimental fragmentation measurements. As the process is markedly anisotropic, such a model can provide only a rough estimate of the accuracy of the cross sections with respect to the experimental situation. The results presented in Table III and Fig. 7 may drive, however, an interesting qualitative discussion. For the C^{2+}-uracil system,

TABLE III. Average of the charge-transfer cross sections for the series of C^{q+}-uracil, $q=[2-4]$, collisional systems.

Velocity (a.u.)	Lab. energy (keV)	Average cross sections (10^{-16} cm^2)		
		$C^{2+}+U$	$C^{3+}+U$	$C^{4+}+U$
0.1	3	0.006	0.163	3.828
0.2	12	0.089	0.064	4.096
0.3	27	0.106	0.029	2.912
0.4	48	0.085	0.017	3.398
0.5	75	0.066	0.011	3.703
0.6	108	0.057	0.007	3.506
0.7	147	0.071	0.005	3.140

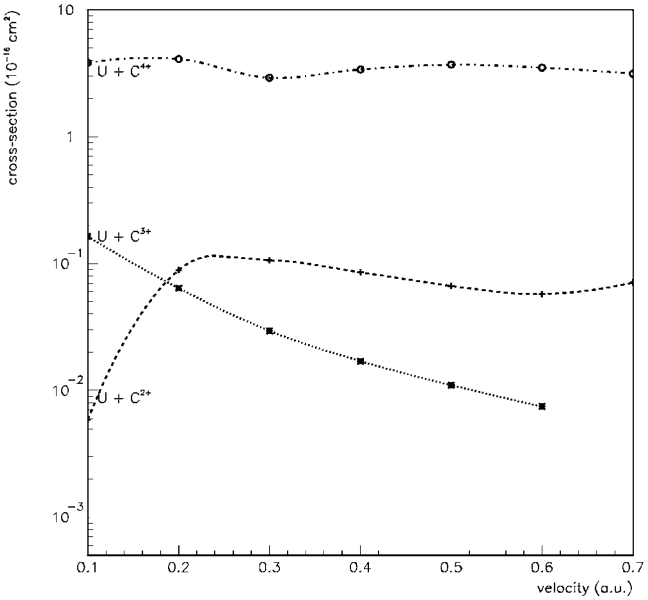

FIG. 7. Average of the charge-transfer cross sections for the C^{q+}-uracil systems.

the charge-transfer cross section is very small, of the order of 0.6×10^{-18} cm^2 at v=0.1 a.u. (E_{lab}=3 keV), in quite good agreement with the experimental measurements which assume almost complete fragmentation of the uracil molecule in that case. The relative yield for fragmentation is then shown experimentally to decrease with increasing impact velocity, which is corroborated by the first increase of the charge-transfer cross section. For higher velocities, the charge-transfer cross section of C^{2+}-uracil remains more or less constant, around 0.1×10^{-16} cm^2. The behavior of the C^{4+}-uracil collision system appears quite different, with only small variations of charge-transfer cross sections with velocity, around $[3.0-4.0]\times10^{-16}$ cm^2, which is corroborated by fragmentation experiments which show lower fragmentation yield than for C^{2+}-uracil, and thus the possibility to have significant charge transfer in that case, considering these processes as complementary. The C^{3+}-uracil charge-transfer cross sections are very small, $[0.01-0.1]\times10^{-16}$ cm^2, the same order of magnitude as calculated for C^{2+}-uracil, and decrease regularly with increasing velocity. The global variation is in accordance with the experimental measurements, which show a regular increasing yield for fragmentation in the velocity range of interest, but we should expect a quite higher order of magnitude if one considers the fragmentation and charge-transfer processes only. The ionization process could possibly be significant for this doublet system, with a singly occupied $2p$ orbital on oxygen, relatively high in energy. Anyway, this discussion shows with a quite significant accuracy that the fragmentation and charge-transfer processes may be considered as complementary with regard to the variation with impact energy. Besides, this work provides an order of magnitude of absolute charge-transfer cross sections.

IV. CONCLUDING REMARKS

We present in this study a simple model for the charge-transfer C^{q+}-uracil (q=[2–4]) reaction. The planar and perpendicular attack of the C^{q+} projectile towards the uracil target is investigated using *ab initio* potential energy curves and couplings followed by a semiclassical collisional treatment. This work shows clearly a strong delocalization of the π electrons of the uracil ring towards the C^{q+} ion, leading to a real chemical bond between the O(4) oxygen and the colliding ion in planar collisions. The variations of the charge-transfer cross sections with the collision velocity are shown to corroborate with a reasonable accuracy the experimental fragmentation measurements in the case of the C^{2+}- and C^{4+}-uracil systems. The process appears to be strongly anisotropic, in particular for the C^{4+} colliding ion. The fragmentation and charge-transfer processes appear to be complementary. A complete approach should take into account simultaneously the ionization process, even if this should not be determinant at such energies. The consideration of internal motions of the uracil target should also be investigated.

ACKNOWLEDGMENTS

The computing facilities of IDRIS (Project No. 51566) are gratefully acknowledged as well as the support of the COST action P9 "Radiation Damage in Biomolecular Systems."

---

[1] C. von Sonntag, in *The Chemical Basis for Radiation Biology* (Taylor & Francis, London, 1987).
[2] B. D. Michael and P. D. O'Neill, Science **287**, 1603 (2000).
[3] B. Boudaiffa, P. Cloutier, D. Hunting, M. A. Huels, and L. Sanche, Science **287**, 1658 (2000).
[4] M. A. Huels, I. Hahndorf, E. Illenberger, and L. Sanche, J. Chem. Phys. **108**, 1309 (1998).
[5] S. Denifl, S. Ptasinska, M. Cingel, S. Matejcik, P. Scheier, and T. D. Märk, Chem. Phys. Lett. **377**, 74 (2003).
[6] H. Abdul-Carime, M. A. Huels, F. Brüning, E. Illenberger, and L. Sanche, J. Chem. Phys. **113**, 2517 (2000).
[7] J. de Vries, R. Hoekstra, R. Morgenstern, and T. Schlathölter, J. Phys. B **35**, 4373 (2002).
[8] J. de Vries, R. Hoekstra, R. Morgenstern, and T. Schlathölter, Eur. Phys. J. D **24**, 161 (2003).
[9] R. Brédy, J. Bernard, L. Chen, B. Wei, A. Salmoun, T. Bouchama, M. C. Buchet-Poulizac, and S. Martin, Nucl. Instrum. Methods Phys. Res. B (to be published).
[10] B. Coupier, B. Farizon, M. Farizon, M. J. Gaillard, F. Gobet, N. V. de Castro Faria, G. Jalbert, S. Ouaskit, M. Carré, B. Gstir, G. Hanel, S. Denifl, L. Feketeova, P. Scheier, and T. D. Märk, Eur. Phys. J. D **20**, 459 (2002).
[11] J. de Vries, R. Hoekstra, R. Morgenstern, and T. Schlathölter, Phys. Rev. Lett. **91**, 053401 (2003).
[12] T. Schlathölter, R. Hoekstra, and R. Morgenstern, Int. J. Mass Spectrom. Ion Process. **233**, 173 (2004).

[13] L. Salem, *Electrons in Chemical Reactions: First Principles* (Wiley Interscience, New York, 1982).
[14] M. C. Bacchus-Montabonel, D. Talbi, and M. Persico, J. Phys. B **33**, 955 (2000).
[15] N. Russo, M. Toscano, and A. Grand, J. Phys. Chem. B **105**, 4735 (2001).
[16] N. Russo, M. Toscano, and A. Grand, J. Am. Chem. Soc. **123**, 10272 (2001).
[17] N. Russo, M. Toscano, and A. Grand, J. Phys. Chem. **107**, 11533 (2003).
[18] N. Russo, E. Sicilia, M. Toscano, and A. Grand, Int. J. Quantum Chem. **90**, 903 (2002).
[19] N. Russo, M. Toscano, and A. Grand, J. Mass Spectrom. **38**, 265 (2003).
[20] Al M. Lamsabhi, M. Alcani, O. Mó, and M. Yanez, Chem Phys Chem **4**, 1011 (2003).
[21] M. C. Bacchus-Montabonel, Phys. Rev. A **59**, 3569 (1999).
[22] L. F. Errea, J. D. Gorfinkiel, C. Harel, H. Jouin, A. Macias, L. Méndez, and A. Riera, Phys. Scr. **T62**, 33 (1996).
[23] L. F. Errea, J. D. Gorfinkiel, E. S. Kryachko, A. Macias, L. Méndez, and A. Riera, J. Chem. Phys. **106**, 172 (1997).
[24] P. C. Stancil, B. Zygelman, and K. Kirby, in *Photonic, Electronic, and Atomic Collisions*, edited by F. Aumayr and H. P. Winter (World Scientific, Singapore, 1998).
[25] MOLPRO (version 2002.1) is a package of *ab initio* programs written by H. J. Werner and P. Knowles with contributions from J. Almlöf, R. D. Amos, A. Berning, D. L. Cooper, M. J. O. Deegan, A. J. Dobbyn, F. Eckert, S. T. Elbert, C. Hampel, R. Lindh, A. Lloyd, W. Meyer, A. Nicklass, K. Peterson, R. Pitzer, A. J. Stone, P. R. Taylor, M. E. Mura, P. Pulay, M. Schütz, H. Stoll, and T. Thorsteinsson.
[26] K. B. Wiberg, R. E. Stratman, and M. J. Frisch, Chem. Phys. Lett. **297**, 60 (1998).
[27] N. Russo, M. Toscano, and A. Grand, J. Comput. Chem. **21**, 1243 (2000).
[28] C. E. Crespo-Hernandez, R. Arce, Y. Ishikawa, L. Gorb, J. Leszczynski, and D. M. Close, J. Phys. Chem. A **108**, 6373 (2004).
[29] V. M. Orlov, A. N. Smirnov, and Y. M. Varshavsky, Tetrahedron Lett. **48**, 4377 (1976).
[30] B. I. Verkin, L. F. Sukodub, and I. K. Yanson, Dokl. Akad. Nauk SSSR **228**, 1452 (1976).
[31] P. Sobocinski, J. Rangama, G. Laurent, L. Adoui, A. Cassimi, J. Y. Chesnel, A. Dubois, D. Hennecart, X. Husson, and F. Frémont, J. Phys. B **35**, 1353 (2002).
[32] R. J. Allan, C. Courbin, P. Salas, and P. Wahnon, J. Phys. B **23**, L461 (1990).